In vitro dual activity of *Aloe marlothii* roots and its chemical constituents against *Plasmodium falciparum* asexual and sexual stage parasites

Sephora Mutombo Mianda[a], Luke Invernizzi[a], Mariëtte E. van der Watt[b,c], Janette Reader[b], Phanankosi Moyo[a,b], Lyn-Marié Birkholtz[b,*], Vinesh J. Maharaj[a,*]

[a] Department of Chemistry, Faculty of Natural and Agricultural Sciences, University of Pretoria, Pretoria 0028, South Africa
[b] Department of Biochemistry, Genetics and Microbiology, Institute for Sustainable Malaria Control, University of Pretoria, Hatfield, Pretoria 0028, South Africa
[c] Institute for Sustainable Malaria Control, School of Health Systems and Public Health, University of Pretoria, Gezina, Pretoria 0031, South Africa

Sephora Mutombo Mianda (sephoramianda@gmail.com)
Luke Invernizzi (lukeinvernizzi@gmail.com)
Mariette E. Botha (mariette.vanderwatt@up.ac.za)
Janette Reader (janette.reader@up.ac.za)
Phanankosi Moyo (phanankosimoyo@gmail.com)
Lyn-Marié Birkholtz (lbirkholtz@up.ac.za)
Vinesh J. Maharaj (vinesh.maharaj@up.ac.za)

*Corresponding author (Chemistry): Vinesh J. Maharaj
Tel: +27 (0824665466)
Email address: vinesh.maharaj@up.ac.za
Department of Chemistry
University of Pretoria
Private Bag x 20
Hatfield, 0028

*Corresponding author (Parasitology): Lyn-Marié Birkholtz
Tel: +27 12 420 2479
Email address: lbirkholtz@up.ac.za
Department of Biochemistry, Genetics and Microbiology
University of Pretoria
Private Bag x 20
Hatfield, 0028

Highlights

- *Aloe marlothii* is used in the African traditional medicine for treatment of malaria.
- Aloesaponarin I and aloesaponol IV were isolated from *A. marlothii* roots.
- Aloesaponarin I showed good potency against asexual stages of *Plasmodium falciparum*.
- Aloesaponol IV displayed pronounced activity against late-stage gametocytes.
- *In silico* studies identified β-hematin and DNA topoisomerase II as potential targets.

Abstract

Ethnopharmacological relevance: *Aloe marlothii* A.Berger (Xanthorrhoeaceae) is indigenous to southern African countries where its aqueous preparations are used in traditional medicine to treat several ailments including hypertension, respiratory infections, venereal diseases, chest pain, sore throat and malaria.

Aim of the study: The aims of this study were as follows: (i) isolate and identify the antiplasmodial active compounds in *A. marlothii* roots. As the water extract was previously inactive, the dichloromethane:methanol (DCM:MeOH) (1:1) was used, (ii) examine the activity of the isolated compounds against *Plasmodium falciparum* asexual blood stage (ABS) parasites as well as for transmission-blocking activity against gametocytes and gametes, and (iii) to use *in silico* tools to predict the target(s) of the active molecules.

Materials and Methods: The crude DCM:MeOH (1:1) extract of *A. marlothii* roots was fractionated on a reverse phase C8 column, using a positive pressure solid-phase extraction (ppSPE) workstation to produce seven fractions. The resulting fractions and the crude DCM:MeOH extract were tested *in vitro* against *P. falciparum* (NF54) ABS parasites using the malaria SYBR Green I based-fluorescence assay. Flash silica chromatography and mass-directed preparative high-performance liquid chromatography were utilised to isolate the active compounds. The isolated compounds were evaluated *in vitro* against *P. falciparum* asexual (NF54 and K1 strains) and sexual (gametocytes and gametes) stage parasites. Molecular docking was then used for the *in silico* prediction of targets for the isolated active compounds in *P. falciparum*.

Results: The crude extract and two SPE fractions displayed good antiplasmodial activity with >97% and 100% inhibition of ABS parasites proliferation at 10 and 20 μg/mL, respectively. Following UPLC-MS analysis of these active fractions, a targeted purification resulted in the isolation of six compounds identified as aloesaponol I (**1**), aloesaponarin I (**2**), aloesaponol IV (**3**), β-sorigenin-1-*O*-methylether (**4**), emodin (**5**), and chrysophanol (**6**). Aloesaponarin I (**2**) was the most bioactive, compared to other isolated constituents, against *P. falciparum* ABS parasites exhibiting equipotency against the drug-sensitive (NF54) (IC_{50} = 1.54 μg/mL (5 μM)) and multidrug-resistant (K1) (IC_{50} = 1.58 μg/mL (5 μM)) strains. Aloesaponol IV (**3**) showed pronounced activity against late-stage (>90% stage IV/V) gametocytes (IC_{50} = 6.53 μg/mL (22.6 μM)) demonstrating a 3-fold selective potency towards these sexual stages compared to asexual forms of the parasite (IC_{50} = 19.77 ± 6.835 μg/mL (68 μM)). Transmission-blocking potential of aloesaponol IV (**3**) was validated by *in vitro* inhibition of exflagellation of male gametes (94% inhibition at 20 μg/mL). *In silico* studies identified β-hematin and DNA topoisomerase II as potential biological targets of compounds **2** and **3**, respectively.

Conclusion: The findings from our study substantiate the traditional use of *A. marlothii* to treat malaria. To our knowledge, this study has provided the first report on the isolation and identification of antiplasmodial compounds from *A. marlothii* roots. Furthermore, our study has provided the first report on the transmission-blocking potential of one of the compounds from the genus *Aloe,* motivating for the investigation of other species within this genus for their potential *P. falciparum* transmission-blocking activity.

Graphical abstract

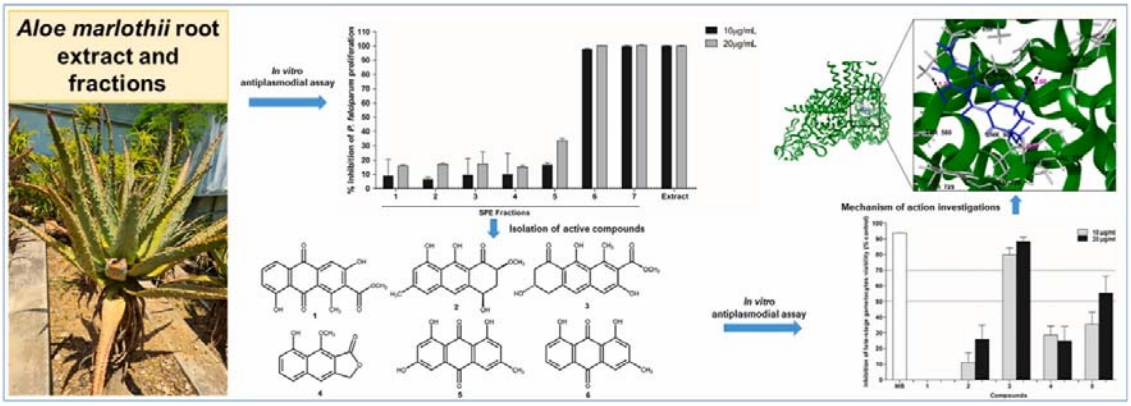

Key words: *Aloe marlothii*, anthraquinones, *Plasmodium falciparum*, antiplasmodial, gametocytocidal, gametocidal, transmission-blocking

1. Introduction

Plasmodium falciparum is one of the five protozoan parasites known to cause malaria in humans (Sato, 2021). It is the most virulent and major cause of severe malaria (WHO, 2021) in patients, while also accounting for the highest number of casualties in the World Health Organisation African Region (WHO, 2021). The *Plasmodium* parasite has a very complex multistage life cycle, occurring in both the human host and female *Anopheles* mosquito vector (Sinha et al., 2014). In the human, the parasite goes through several asexual stages, including an exo-erythrocytic phase (occurring in the liver) and an intra-erythrocytic stage (in the bloodstream). However, in the course of the parasite's asexual proliferation in the bloodstream, a small portion (<10% of the total asexual parasite population) will commit and differentiate through five morphologically distinct sexual developmental stages (stages I–V) of *Plasmodium*, known as the gametocytes. Mature stage V male (micro-) and female (macro-) gametocytes are terminally differentiated and the only stage of *P. falciparum* that supports transmission from the human host to mosquito vector. Inside the mosquitoes' midgut, micro-gametocytes differentiate into microgametes in a process called exflagellation, while macro-gametocytes form macro-gametes. Micro- and macro-gametes fuse to form a diploid zygote that develops into a motile ookinete. Ookinetes penetrate the midgut wall where they form oocysts which enlarge overtime and eventually rupture to release sporozoites. The sporozoites migrate to the mosquito salivary glands ready to infect a human on collection of a blood meal (Cox, 2010). Malaria eradication has become the ambitious goal of global malaria programs, rather than control. Therefore, for new antimalarial candidates, emphasis is placed upon molecules with the additional ability to block human-to-mosquito transmission of the parasite. Hence, candidates able to cure, by targeting the intra-erythrocytic asexual blood stage (ABS) forms of *Plasmodium* (Target candidate profile (TCP)-1), ideally, need to also target sexual gametocyte forms (TCP-5) in order to prevent human-to-mosquito and mosquito-to-human parasite transmission (Alonso et al., 2011; Birkholtz et al., 2016, Birkholtz et al., 2022; Burrows et al., 2017; Moyo et al., 2020).

Aloe marlothii A.Berger (Xanthorrhoeaceae), also called mountain aloe, flat-flowered aloe (English), bergalwyn (Afrikaans) and umhlaba (Zulu), is a perennial, single-stemmed, large and succulent aloe species growing in Botswana, Mozambique, South Africa, Swaziland and

Zimbabwe. The leaves are large and broad with spines covering their upper and lower surfaces and maroon coloured indentations and orange tips alongside leaf edges (SANBI, 2007). *Aloe* species are used in folk medicine for the treatment of several ailments in various preparations. Decoctions prepared from *Aloe* species leaves are taken orally three times a day to treat malaria and fever in Namibia (Mulyangote, 2016). The leaf juice and sap of several *Aloe* species are reported for their use in the treatment of malaria in many African countries (Nguta et al., 2010; Wabuyele and Kyalo, 2008), whereas in Togo and Cote d'Ivoire, the roots of *A. buettneri* are used for this purpose (Schmelzer and Gurib-Fakim, 2008). *A. marlothii* leaves and roots are utilised singularly or mixed with other species for the treatment of hypertension (de Wet et al., 2016), tuberculosis, venereal diseases (Erasmus et al., 2012), hair treatment (Nicosia et al., 2020), chest pain, sore throat, pneumonia (Semenya and Mokgoebo, 2020), diabetes (Semenya et al., 2012), diarrhoea and gall sickness in livestock (Khunoana et al., 2019; Ndlela et al., 2021). The sap of *A. marlothii* leaves are administered orally by the local community in the Canhane village, in Mozambique, to treat malaria (Ribeiro et al., 2010).

Several *Aloe* species have been evaluated for their antiplasmodial activity and many of them have shown moderate to good activities *in vitro* against ABS of various drug-sensitive and -resistant strains of *P. falciparum* and *P. berghei* with IC_{50} values as low as 3.5 μg/mL in some cases (Amoo et al., 2014; Bbosa et al., 2013; Deressa et al., 2010; Dibessa et al., 2020; Hintsa et al., 2019; Teka et al., 2020; Tewabe and Assefa, 2018; van Zyl et al., 2002). Most studies were conducted on leaves and numerous compounds (mainly anthrones) were isolated and evaluated against *P. falciparum* ABS parasites (Geremedhin et al., 2014; Paulos et al., 2011; Teka et al., 2016). *A. marlothii*, similarly to other *Aloe* species, has been subjected to various antiplasmodial studies examining its potency against *Plasmodium* ABS parasites. In one study, the aqueous and organic extracts of *A. marlothii* leaves and whole plants were evaluated *in vitro* against the chloroquine-sensitive *P. falciparum* D10 strain. The dichloromethane (DCM) extract of *A. marlothii* whole plant displayed the best activity with an IC_{50} value of 3.5 μg/mL (Clarkson et al., 2004). In another study, the methanol (MeOH) extract of *A. marlothii* roots was evaluated *in vitro* and was shown to be potent against *P. falciparum* (FCR-3) ABS parasites (van Zyl et al., 2002). Despite the notable activity of crude *A. marlothii* extracts against *P. falciparum* ABS parasites, the active ingredients have not been identified to our knowledge. Nonetheless, various anthraquinones and pre-anthraquinones have been extracted from the roots and stems of several *Aloe* species and tested against *P. falciparum*. Among them, aloesaponarin I, aloesaponarin II and laccaic acid D-methyl ester (Hou et al., 2009, Wanjohi, 2005) showed good antiplasmodial activity with IC_{50} below 5 μg/ml. However, none of the compounds isolated from *Aloe* species have been investigated for their transmission-blocking potential by assessing their activity against either *P. falciparum* gametocytes or gametes. In this context, we explored the antiplasmodial activity of *A. marlothii*, and, aided by advanced hyphenated analytical techniques, endeavoured to identify the active constituents. Herein, we provide a first report on the isolation of six compounds from the roots of *A. marlothii* and present data on their *in vitro* activity against the intra-erythrocytic asexual and sexual forms of *P. falciparum*. Furthermore, we provide insights into possible biological targets and mode of action (MoA) of the most active antiplasmodial compounds isolated from *A. marlothii* roots.

2. Material and methods

2.1 General

Fractionation of crude extract was carried out on a positive pressure solid phase extraction (ppSPE) workstation (Gilson GX-241 Liquid Handler, WI, USA) using a reverse phase C8 column (Thermo Scientific, Hypersep C8, 2g/6mL). The workstation was controlled using Trilution® LH v4.0.4.0 software (Trilution, Gilson, United Kingdom). 96 Deep well plates for storage and copy for biological evaluation were prepared using a customized, high-throughput automated protocols implemented on Hamilton Microlab STARlet liquid handler (Hamilton Life Sciences). Plates were kept in a Hamilton automated sample storage freezer (Verso® Q20 for Promolab). Further purification was carried out on a BUCHI Pure C-815-Flash system using BUCHI prepacked flash silica columns procured from Labotech (Gauteng, South Africa). Preparative high-performance liquid chromatography (HPLC) was carried out on a Waters chromatographic system equipped with a photodiode array (PDA) detector (Model 2998) and interphased with an Acquity QDa detector (Waters, Milford, MA, USA). Preparative HPLC separation was achieved on an XBridge Prep C_{18} column (19 x 250 mm, 5 μM, Waters). Analytical and technical grade solvents used in extraction, fractionation and preparative HPLC were procured from Merck South Africa (Merck, Darmstadt, Germany) and Romil-SpS™, Microsep, South Africa (Waterbeach, Cambridge, United Kingdom). All solvents were used without further treatment. The *Pfs* 25 specific antibody was obtained through BEI Resources, NIAID, NIH: Monoclonal Anti-Plasmodium falciparum 25-kDa Gamete Surface Protein (*Pfs* 25), Clone 4B7 (produced *in vitro*), MRA-28, contributed by Louis H. Miller and Allan Saul. The antibody was labelled using a fluorescein isothiocyanate (FITC) dye (Thermo Scientific) as per manufacturer's protocol. For florescence microscopy, a Carl Zeiss Axio Lab. A1 Fluorescence microscope with a 100X oil immersion and 10X objectives was used. This had been fitted with a Zeiss Axiocam 202 mono camera linked to a computer with ZEN 3.0 Blue Edition software.

2.2 Plant material and extraction

In the previous study, the water extract, which was the classical traditional preparation of *A. marlothii*, did not show any activity against *P. falciparum* (Clarkson et al., 2004), the DCM:MeOH (1:1) extract was therefore selected for this study. The crude DCM:MeOH (1:1) extract of *A. marlothii* roots used was retrieved from the University of Pretoria repository in the Department of Chemistry at the University of Pretoria. This was from a batch of extracts previously prepared by Clarkson *et al.* (Clarkson et al., 2004) using sequential extraction of dried *A. marlothii* roots (Voucher specimen (BP00049) deposited at the National Herbarium of the South African Biodiversity Institute). The plant taxa were checked and confirmed on http://www.theplantlist.org/.

To facilitate the isolation of active compounds, fresh large quantities of *A. marlothii* root plant material was collected from the Manie van der Schijff Botanical Garden, at the University of Pretoria Hatfield campus in February 2021 with the help of the University's curator, Jason Samuels. A voucher specimen was prepared and deposited at the H.G.W.J. Schweickerdt Plant Herbarium at the University of Pretoria (Voucher specimen code: PRU 128789).

The roots were dried in the oven at 60˚C for one week. Dried plant material was ground to a fine powder by using a grinder (Polymix, PX-MFC 90 D, Lasec, Gauteng, South Africa). The dried roots of *A. marlothii* (860 g) were exhaustively extracted with DCM:MeOH (1:1) at room temperature. The extract was concentrated under vacuum to yield a dry crude extract.

2.3 Fractionation of crude *A. marlothii* extract

The extract (160 mg) was fractionated using a ppSPE workstation on a reverse phase C8 cartridge with the eluent of water (H_2O), MeOH and acetonitrile (MeCN) in the following ratios: for fractions 1 to 6: H_2O:MeOH 95:5, 80:20, 60:40, 40:60, 20:80, 0:100, respectively, and for fraction 7: MeOH:MeCN 50:50. The fractions (SPE fractions 1-7) were collected (8 mL each) in pre-weighed 10 mL polypropylene 2D-barcoded tubes. Using a Hamilton Microlab STARlet robotic liquid handler, 800 µL of each fraction was transferred from the 2D-barcoded tubes to a 96 deep well plate (SPE Fraction 1-7 in wells 1 to 7, respectively, while the extract was placed in well 8). The solvents were evaporated to dryness from the 96 deep well plate and the 2D-barcoded tubes using a Genevac HT Series (Genevac Ltd., Ipswich, United Kingdom). The loaded dry 2D-barcoded tubes were weighed and the masses of fractions were recorded on a comma separated values Microsoft Excel document used as input file on the liquid handler, which enabled the instrument (liquid handler) to calculate and transfer the necessary volume of 100% dimethyl sulphoxide (DMSO) (Sigma-Aldrich) to each well of the 96 deep well plate containing the dry fractions and extract in order to obtain a final stock concentration of 5 mg/mL. Lastly, the extract and fractions were transferred from the 96 deep well plate into FluidX 96-format tubes (mother plate, 1.0 mL tri-coded tube, external thread) for cold storage in a robotic freezer for the University of Pretoria Natural Product library. For the preparation of a copy plate for antiplasmodial evaluation, the mother plate was retrieved from the freezer, thawed and 100 µL of each fraction and extract transferred to a new 96 deep well plate using the liquid handler. The resulting copy was submitted for biological assessment, while the mother plate was returned for storage in the freezer.

2.4 *In vitro* assessment of the antiplasmodial activity of crude extract and SPE fractions against *P. falciparum* ABS parasites

The extract and SPE fractions of *A. marlothii* roots were subjected to antiplasmodial *in vitro* activity assessment against *P. falciparum* NF54 (drug-sensitive) ABS parasites using the malaria SYBR Green I-based fluorescence assay (Johnson et al., 2007; Smilkstein et al., 2004; Verlinden et al., 2011). Parasitology work and volunteer human blood donation at the University of Pretoria is covered under ethical approval from the Health Sciences Ethics Committee (506/2018) and Natural and Agricultural Sciences Ethics Committee (180000094) to LB. The *P. falciparum* parasites were maintained at 37˚C in human erythrocytes (O^+) suspended in complete culture medium [RPMI 1640 medium (Sigma-Aldrich) supplemented with 25 mM HEPES (Sigma-Aldrich), 20 mM D-glucose (Sigma-Aldrich), 200 µM hypoxanthine (Sigma-Aldrich), 0.2% (w/v) sodium bicarbonate, 24 µg/mL gentamycin (Sigma-Aldrich) and 0.5% (w/v) AlbuMAX II] in a hypoxic atmosphere of 90% N_2, 5% O_2 and 5% CO_2. The culture was synchronised using D-sorbitol (5% w/v) to achieve an >95% homogenous ring-stage ABS culture. For primary evaluation, dual point assays (one biological experiment (n = 1) carried out in technical triplicates) were performed with 10 and 20 µg/mL of the extract and SPE fractions (concentration selected based on the classification criteria for antiplasmodial activity of plant extracts find in the paper published by Moyo *et al.* (Moyo et al., 2016)). *P. falciparum* NF54 (drug sensitive) ABS parasites (100 µL, 1%

parasitaemia and 2% haematocrit) were treated with an equal volume of either the crude extract or SPE fractions in sterile 96 well plates, for 96 h at 37°C under hypoxic conditions. The SYBR Green I fluorescence was determined as before (Johnson et al., 2007; Smilkstein et al., 2004; Verlinden et al., 2011). Data were analysed as mean ± S.D. Chloroquine (1 μM) served as a positive control for inhibition of parasite proliferation.

2.5 UPLC-QTOF-MS analysis of *A. marlothii* extract and active SPE fractions

Following antiplasmodial evaluation, the most potent fractions were subjected to qualitative analysis using hyphenated analytical techniques to tentatively identify the potentially active constituents in *A. marlothii* roots and guide their isolation. The active fractions were subjected to analysis using an ultra-performance liquid chromatography quadrupole-time-of-flight mass spectrometer (UPLC-QTOF-MS). In order to carry out this analysis, the samples (extract and selected SPE fractions) were prepared at a concentration of 1 mg/mL by dissolving them in MeOH. They were run on a Waters Acquity UPLC System equipped with a binary solvent delivery system and an autosampler. The Waters BEH C18 (2.1 mm x 100 mm, 1.7 μm) column was used. The mobile phase consisted of solvents A = H_2O + 0.1% formic acid and B = MeOH + 0.1% formic acid, applied in gradient mode (0 min 3% B, 0.10 min 3% B, 14 min 100% B, 16 min 100% B, 16.5 min 3% B, 20 min 3% B) with a flow rate of 0.3 mL/min. The injection volume was 5 μL. The separated compounds were analysed by a QTOF mass spectrometer, which was run in electrospray ionization (ESI) positive and negative modes. Compounds were tentatively identified by generating the respective molecular formula from MassLynx V 4 and comparing them with published data, including the fragmentation patterns. From this analysis step, compounds belonging to the class anthraquinones, were identified, and hypothesised to be responsible for the observed biological activity. These compounds were subsequently prioritised for isolation.

2.6 Isolation of antiplasmodial compounds

The DCM:MeOH (1:1) crude extract was subjected to solvent-solvent partitioning between H_2O:MeOH (10:90) and *n*-hexane (*n*-hex). Both fractions were dried under vacuum and were subjected to HPLC-MS analysis. Based upon this analysis the two partitioned fractions were treated as follows.

(i) A portion of the H_2O:MeOH fraction was purified by using mass-directed preparative-HPLC on an XBridge preparative C18 column (19 mm × 25 mm, i.d., 5 μm particle size, Waters), flow rate 20 mL/min, mobile phase 0.1% formic acid in H_2O (solvent A) and MeCN (solvent B), using a linear gradient (0 min 5% B, 1.67 min 5% B, 30 min 100% B, 34 min 100% B, 36 min 5% B, 38 min 5% B) to give compound **2** (retention time: 21.00 min) and five sub-fractions (F1 to 5). The sub-fraction F4 (retention time: 11.77 min) was further resolved on the same XBridge preparative C18 column, flow rate 20 mL/min, mobile phase 0.1% formic acid in H_2O (solvent A) and MeCN (solvent B), with a linear gradient (0 min 25% B, 1.67 min 25% B, 30 min 60% B, 34 min 100% B, 36 min 100% B, 37 min 25% B, 38 min 5% B) yielding compound **3** (retention time: 17.58 min).

(ii) The remaining portion of the H_2O:MeOH fraction and the *n*-hex fraction were separately purified using a flash chromatography system (BUCHI Pure C-815 Flash), on a prepacked silica column FP EcoFlex Si 120 g and 80 g, respectively, with 50 μm irregular particle size. The flow

rates were set to 85 and 60 mL/min, respectively. The eluents were *n*-hex and ethyl acetate (EtOAc) in a slope gradient mode starting from 0 to 100% EtOAc. The run times were 100.6 min for H_2O:MeOH fraction and 134.4 min for *n*-hex fraction. Compounds were detected by UV and ELSD detectors as they eluted from the column. After combining similar sub-fractions, a total of 60 sub-fractions (called H_2O:MeOH sub-fractions) were collected from the H_2O:MeOH fraction and 19 sub-fractions (called *n*-hex sub-fractions) from the *n*-hex fraction. All fractions were submitted for HPLC-MS analysis. Based on this analysis, the H_2O:MeOH sub-fraction 32 and *n*-hex sub-fractions 4 and 9 were selected for further purification primary as they contained the target compounds (the anthraquinones).

The H_2O:MeOH sub-fraction 32 was purified by using mass-directed preparative HPLC on an XBridge preparative C18 column (19 mm × 25 mm, i.d., 5 μm particle size, Waters), flow rate 20 mL/min, mobile phase 0.1% formic acid in H_2O (solvent A) and MeCN (solvent B), using a linear gradient (0 min 5% B, 1.67 min 5% B, 30 min 100% B, 34 min 100% B, 36 min 5% B, 38 min 5% B) which afforded compound **1** (retention time: 15.32 min).

The *n*-hex sub-fractions 4 and 9 obtained from *n*-hex fraction were purified on preparative HPLC, on XBridge preparative C18 column, flow rate 20 mL/min, mobile phase 0.1% formic acid in H_2O (solvent A) and MeCN (solvent B) with a linear gradient (0 min 20% B, 1.67 min 20% B, 30 min 100% B, 34 min 100% B, 36 min 20% B, 38 min 20% B) to give compound **4** (retention time 13.53 min, from *n*-hex sub-fraction 9), compound **6** (retention time 22.73 min, from *n*-hex sub-fraction 4), and compound **5** (retention time 24.47 min, from *n*-hex sub-fraction 4).

2.7 UPLC-QTOF-MS analysis of isolated compounds

The six isolated compounds were analysed using the UPLC-QTOF-MS operating in the ESI positive and negative modes to resolve their exact masses as described earlier in this manuscript.

2.8 NMR analysis of isolated compounds

1D and 2D NMR spectra of the six isolated compounds were recorded at room temperature on Bruker AVANCE III 500 MHz spectrometer. Deuterated solvents were used to dissolve the compounds, deuterated methanol (CD_3OD) (Merck), deuterated dichloromethane (CD_2Cl_2) (Sigma-Aldrich) and deuterated chloroform ($CDCl_3$) (Sigma-Aldrich). The chemical shifts are reported in ppm (δ-scale) and the calibrations of the spectra were done by using the trace protons from the deuterated solvents, for CD_3OD = δ_H – 3.31 and δ_C – 49.1, $CDCl_3$ = δ_H – 7.26 and δ_C – 77.16 and CD_2Cl_2 = δ_H – 5.32 and δ_C – 54.00. The coupling constants "*J*" are given in Hertz (Hz).

2.9 Dose-response evaluation of isolated compounds against *P. falciparum* (NF54 and K1) ABS parasites

The isolated compounds were subjected to *in vitro* evaluation against *P. falciparum* drug-sensitive (NF54) and K1 (multidrug-resistant) ABS as before, but full dose-response was determined. A concentration range of 0.156 to 40 μg/mL were evaluated with 2-fold serial dilution over 9 concentration points. Two biological repeat assays in technical triplicates were performed for each of the five isolated compounds. Chloroquine served as a positive control. Sigmoidal dose-response analyses were performed using GraphPad Prism (v5) to determine the concentration required to inhibit proliferation of 50% of the culture (IC_{50}). Results are reported as mean ± S.E.M.

2.10 *In vitro* assessment of the gametocytocidal and gametocidal activity of isolated compounds

To assess the effect of the isolated compounds against late-stage NF54-*Pfs*16-GFP-luc gametocytes (>90% stage IV/V, 2% gametocytaemia), the luciferase assay was used as described by Reader *et al.* (Reader et al., 2015). Primary dual point analysis (at 10 and 20 μg/mL, $n = 1$, in technical triplicates) preceded full dose-response investigations (9-point concentration, 2-fold serial dilution over concentration range of 0.156 to 40 μg/mL, $n = 2$ in technical triplicates). Methylene blue (5 μM) was used as a positive control for the inhibition of *in vitro* gametocyte viability. Data analysis and determination of IC_{50} were carried out in GraphPad Prism (v5). Results are reported as mean ± S.E.M.

To validate the transmission-blocking activity of the compounds, a dual gamete formation assay (DGFA) was performed on female (female gametocyte activation) and male gametes (exflagellation inhibition assay (EIA)) (Reader et al., 2021, Ruecker et al., 2014). The DGFA was performed at 20 μg/mL by exposing mature (stage V) gametocytes (2% gametocytaemia) to compound for 48 h. Drug exposed culture (1 mL) was transferred into a 1.5 mL Eppendorf tube, centrifuged until cells had pelleted following which the supernatant was removed and the parasites resuspended in 200 μL of ookinete medium. From the resuspended culture, 10 μL was used to assess exflagellation as described (Reader et al., 2021). The rest of the resuspended parasites were incubated at room temperature for 24 h, subsequently resuspended in 200 μL anti-*Pfs* 25 monoclonal antibody (labelled with fluorescein isothiocyanate) at a dilution of 1:1000 (PBS) and incubated overnight at 4°C in the dark. The immunostained parasites (10 μL) were visualised with fluorescence microscopy at x100 objective. Images (60 randomly captured) under the green and brightfield channel from which the total number of female gametes were counted. Two independent biological experiments were set up for the DGFA, with methylene blue (10 μM) serving as the positive control.

2.11 *In silico* target prediction

To predict the biological targets of most potent compounds, *in silico* tools were used in a multi-step approach as follows:

(i) Based on prior published data (Osman and Ismail, 2018) indicative of this class of compounds inhibiting hemozoin formation, the most active compound against the *P. falciparum* ABS parasites was docked against the hemozoin crystal lattice to assess potential binding events to this target.

(ii) To predict target for most potent gametocytocidal compound, an unbiased *in silico* target identification approach was utilised. The target was first predicted by submitting the respective simplified molecular-input line-entry system (SMILES) of the active molecule on two different online programmes, the similarity ensemble approach (SEA) (https://sea.bkslab.org/) (Keiser et al., 2007) and SuperPred (https://prediction.charite.de/index.php) (Nickel et al., 2014). The mechanism of action was then assessed further by molecular docking.

Molecular modelling was conducted with the Schrödinger software suite, release 2021-3, employing the OPLS4 forcefield. The ligand structures used were downloaded from the Pubchem database and prepared using ligprep. Ligand protonation states were predicted using Epik

(Greenwood et al., 2010; Shelley et al., 2007) with a target pH set at 7.0 ± 2.0. The protein structure, topoisomerase II, was prepared using Schrödinger's protein preparation wizard, with PRIME utilised to fill in any missing loops and side chains (Jacobson et al., 2004, 2002). Amino acid protonation sites were assigned and energy minimization performed to reduce the overall potential energy of the protein thereby reducing any unfavourable constraints. Hemozoin was generated from the β-hematin anhydride dimer crystal structure previously published (Bohle et al., 2012) and obtained from 'The Cambridge Crystallographic Data Centre' (CCDC) (XETXUP01). A 2x2x2 cell lattice was formed to display the packing and interaction of the dimers in the hemozoin lattice, using Mercury v3.5.1. The hemozoin cell lattice was further imported and prepared with the protein preparation wizard, with zero-order bonds created between the metal and its ligands. Furthermore, all iron (Fe) atom centers were altered to a +3-oxidation state and manual inspection and alteration was done to ensure the atoms of the ligated porphyrin moiety had the correct charge and interactions, corresponding to published literature (Bailly, 2021; Pagola et al., 2000). Protonation states were assigned and energy minimization performed to further relieve any unfavourable constraints. Receptor grids were generated for both the topoisomerase II structure and the hemozoin cell lattice. These were generated using default settings for both topoisomerase II and the hemozoin crystal lattice. The receptor grid was centered at coordinates 40.57, -22.41, 29.03 corresponding to the x, y and z-axis, respectively, for topoisomerase II, close to the site described previously for human topoisomerase II (Wu et al., 2013) and close to a previously used active site for *P. falciparum* (Sol Sol de Medeiros et al., 2021). For the generated hemozoin crystal lattice, the receptor grid was set to encompass the entire hemozoin lattice to ensure docking could occur from any face and centered at coordinates 11.0, 15.0, 7.96 corresponding to the x, y and z-axis, respectively, with the following dimensions (Å): (x, y, z) = (40, 40, 40). Molecular docking was performed using Glide extra precision (XP) (Friesner et al., 2006) with all ligand structures treated as flexible with at least 5 poses generated for each ligand. Post-docking minimisation was done on all poses generated and strain correction terms applied.

3. Results and Discussion

With the goal of eliminating malaria, emphasis has been placed on the discovery and development of new antimalarials that ideally demonstrate dual activity i.e. being active against both asexual and sexual forms of *Plasmodium* parasites. This has triggered concerted efforts to investigate different drug sources in search of potent compounds with TCP-1 and TCP-5 activities (Burrows et al., 2017). The historical success of plant derived natural products in antimalarial drug discovery (Moyo et al., 2020, Wells, 2011), prompted us to search for dual TCP-1 and TCP-5 bioactive compounds from the traditional antimalarial plant *A. marlothii*. Here we report on the *in vitro* potency of its constituents against both *P. falciparum* asexual and sexual parasites. We have also gained insights into the MoA of the active principles.

3.1 *In vitro* inhibition of *P. falciparum* NF54 ABS parasites by the extract and its fractions

The crude DCM:MeOH (1;1) extract and its seven SPE fractions were subjected to *in vitro* antiplasmodial evaluation against drug sensitive *P. falciparum* (NF54) ABS parasites using the SYBR Green I-based assay (Table 1). Chloroquine (1 μM) served as a positive control drug exhibiting 100% (n = 1, in technical triplicates) inhibition of parasite proliferation. From the dual point analysis, the seven fractions and the crude extract showed differential potency against ABS

parasites. The SPE fractions 6 and 7 demonstrated activity comparable with that of the crude extract with 100% inhibition of *P. falciparum* parasites at 20 μg/mL and >97% inhibition (97.77%, 99.89% and 100% for SPE fractions 6, 7 and crude extract, respectively) at 10 μg/mL. Collectively, this data suggested that the active ingredients might be non-polar as the earlier fractions containing polar compounds were not potent, an assumption further supported by a previous report of the antiplasmodial activity of crude methanol (a polar solvent) *A. marlothii* roots extract, which displayed minimal activity (van Zyl et al., 2002). Owing to their activity, the SPE fractions 6 and 7 were prioritised for further investigations.

Table 1: Activity of the crude DCM:MeOH (1:1) extract of *A. marlothii* root and its SPE fractions against *P. falciparum* (NF54) ABS parasites

SPE Fraction	**Mass of fraction (mg)#**	**Inhibition of *P. falciparum* (NF54) parasite proliferation (%)***	
		10 μg/mL	**20 μg/mL**
1	0.8	8.7±11.8	15.9±0.6
2	0.5	6.5±1.5	16.9±0.9
3	0.5	9.5±11.7	17.2±8.4
4	1.4	9.9±14.5	15.0±1.1
5	21	16.9±1.8	33.4±1.7
6	30.6	97.8±0.4	100.3±0.1
7	34.7	99.9±0.6	100.5±0.6
Crude extract	NA	100.0±0.2	100.1±0.3

Mass of SPE fraction realised following the SPE fractionation of the crude extract
* $n = 1$, in technical triplicates
NA – not applicable

3.2 Anthraquinones tentatively identified as possible antiplasmodial compounds in *A. marlothii* roots

The active SPE fractions (6 and 7) and crude extract were analysed by UPLC-QTOF-MS for tentative identification of the active compounds which was achieved through accurate mass determination and fragmentation patterns. The major peak in both the active fractions and the extract was at m/z 317.1104 (Figure 1) and retention time 8.71 min in the first order mass spectrum chromatogram which corresponded to the $[M+H]^+$ ion.

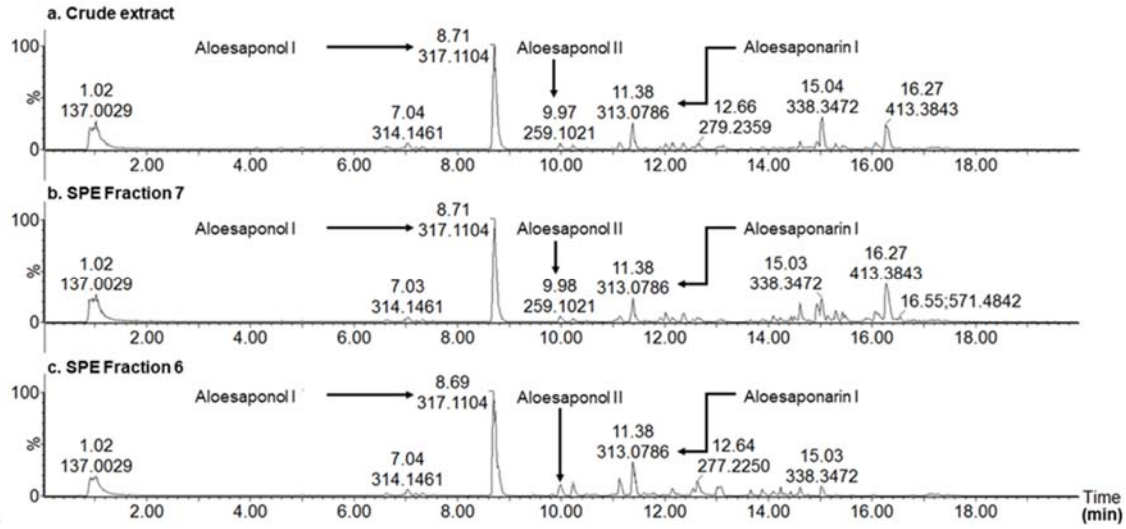

Figure 1: ESI positive-mode BPI chromatogram and chemical characterization of active fractions (SPE fraction 6 and SPE fraction 7) and extract.

The elemental composition of the peak at m/z 317.1104 with retention time 8.81 min generated through MassLynx software algorithm was $C_{17}H_{17}O_6$ with a normalised iFit value of 0.001. The molecular formula matched aloesaponol I (**1**, Figure 2), an anthraquinone, in agreement with previous reports (Wanjohi, 2005). The second major peak was at m/z 313.0786, with retention time 11.38 min and elemental composition of $C_{17}H_{13}O_6$ (normalized iFit = 0.001). This was identified as the anthraquinone aloesaponarin I (**2**, Figure 2) (Wanjohi, 2005). The third major peak was at m/z 259.1021 with retention time 9.97 or 9.98 min and elemental composition of $C_{15}H_{15}O_4$ (normalised iFit value of 0.011, which corresponded to the $[M+H]^+$ ion). The accurate mass of this peak matched two anthraquinones aloesaponol II and prechrysophanol, while the fragmentation pattern closely matched those reported for both as these two compounds have very similar fragmentation pattern (Wanjohi, 2005). Aloesaponol II had previously been detected in the root of *A. marlothii* by using HPLC-UV and TLC and comparing the retention time and R_f to those of a standard (Van Wyk et al., 1995), while prechrysophanol had been isolated from *A. graminicola* (Yenesew et al., 1993). Since anthraquinones are well characterised for their antiplasmodial activity (Osman and Ismail, 2018), a hypothesis was set forth that anthraquinones in *A. marlothii* were responsible for the observed *in vitro* activity. The anthraquinone compounds were subsequently prioritised for isolation from the roots of *A. marlothii*.

3.3 Mass-directed isolation of compounds from *A. marlothii* roots

To isolate the anthraquinone compounds hypothesised to be responsible for the observed antiplasmodial activity, an exhaustive DCM:MeOH (1:1) bulk extraction of *A. marlothii* roots (860 g) was carried out. The resulting crude extract (20 g) was subjected to liquid-liquid partitioning between two solvent systems, H_2O:MeOH (10:90) and *n*-hexane affording 17.76 g and 1.7 g of each fraction, respectively. The two resulting fractions were further investigated for the isolation of the targeted anthraquinones.

The H_2O:MeOH (1.3 g) fraction was subjected to purification using mass directed preparative HPLC-MS, which gave aloesaponarin I (**2**) and five sub-fractions. Sub-fraction (F4) was further resolved on the preparative HPLC-MS to afford compound **3**. An additional portion of the

H_2O:MeOH fraction (5 g) was fractioned using flash silica chromatography. From the 60 sub-fractions collected and analysed by HPLC-MS, sub-fraction 32 was observed to have the targeted compounds. Sub-fraction 32 was further purified using mass directed preparative HPLC-MS resulting in the isolation of aloesaponol I (**1**) (Figure 2).

The *n*-hexane fraction was fractionated using flash silica chromatography yielding 19 sub-fractions among which, two (sub-fractions 4 and 9 observed from the HPLC-MS analysis to have the targeted compounds) were resolved on preparative HPLC-MS to give compounds **4**, **5**, and **6** (Figure 2). Structure elucidation was undertaken on all isolated compounds.

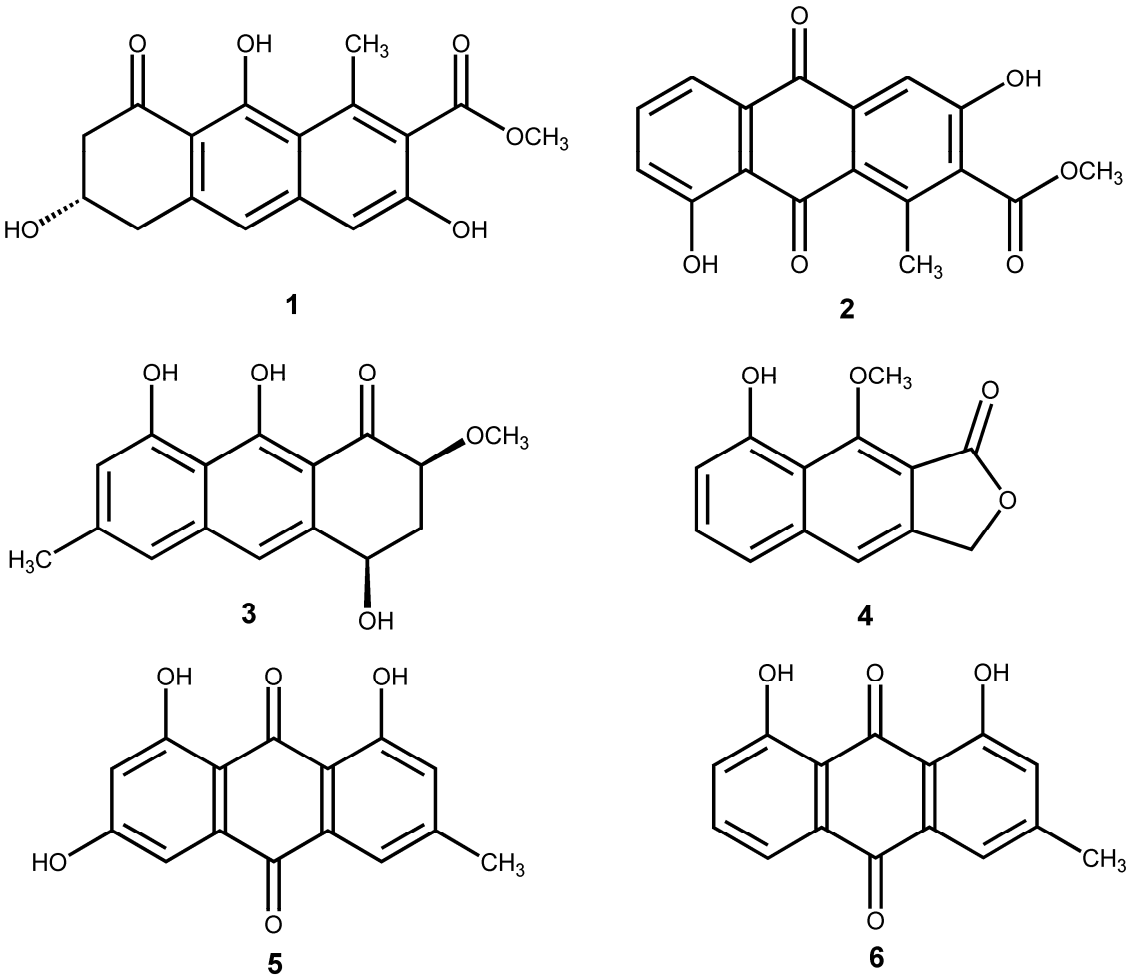

Figure 2: Chemical structures of compounds isolated from *A. marlothii* roots.

Aloesaponarin I (**2**) was isolated as a yellow powder. The molecular formula deduced from its monoprotonated molecular ion at m/z 313.0697 (calcd for $[M+H]^+$ m/z 313.2821) based on the QTOF mass spectrum was $C_{17}H_{12}O_6$. The ^{1}H NMR spectrum exhibited an ABC pattern with three protons resonating at δ_H 7.31 (1H, dd, J = 1.07, 8.31 Hz, H-5), 7.62 (1H, t, J = 8.10 Hz, H-6) and 7.77 (1H, dd, J = 1.07, 7.50 Hz, H-7). The ^{13}C NMR spectrum revealed the presence of 17 carbons with two signals appearing at δ_C 190.1 and 182.7 suggesting the presence of two carbonyls characteristic of the anthraquinone moiety, an additional carbonyl resonating at δ_C 170.6 and two quaternary aromatic oxygenated carbons (δ_C 162.6 and 163.6). The HMBC and COSY correlations

were all in accordance with the compound being the previously reported aloesaponarin I (Abdissa et al., 2017). Aloesaponarin I (**2**) had been detected in the majority of *Aloe* species and hence reported to be one of characteristic components of the *Aloe* genus (Dagne et al., 1994; Van Wyk et al., 1995).

Compound **3** was isolated as a yellow powder. It had a molecular formula of $C_{16}H_{16}O_5$ as deduced from its monoprotonated molecular ion at *m/z* 289.1084 (calcd for $[M+H]^+$ *m/z* 289.1076) based on the QTOF mass spectrum. The ^1H NMR spectrum exhibited three singlets in the aromatic region at δ_H 6.78 (1H, s, H-5), 7.03 (1H, s, H-7) and 7.14 (1H, s, H-10). The position of these protons was assigned through meta COSY interaction between H-5 and H-7, suggesting a meta-coupling (Figure 3). The ^1H NMR spectrum also showed the presence of two oximethine protons resonating at δ_H 4.44 (1H, dd, H-2) and 5.14 (1H, brs, H-4), one methylene group appearing at δ_H 2.37 (1H, dd, H-3) and 2.55 (2H, dd, H-3), one methoxy group at δ_H 3.68 (3H, s, OCH_3-2). Two aromatic hydroxyl groups were appearing at δ_H 9.59 (1H, s, OH-8) and 15.80 (1H, s, OH-9), an assumption further supported by the ^{13}C NMR spectrum, which showed two signals at δ_C 157.95 and 166.49. The position was further confirmed by NOESY interaction between OH-8 and OH-9. The ^{13}C NMR spectrum revealed the presence of 16 carbons with one signal at δ_C 201.72 suggesting a carbonyl group. This indicated that the molecule was a tetrahydroanthracene, which matched aloesaponol IV, previously isolated from *Aloe Saponaria* subterranean stems (Yagi et al., 1977). This supposition was further confirmed by COSY interactions between the methylene protons H-3 with both H-2 and H-4. The absolute configuration was deduced from ^1H NMR spectrum by analysing the coupling constants between H-2 and H-3 (H-2, J_{aa} = 9.6, J_{ae} = 4.41) and H-4 and H-3 (H-4, J_{aa} = 5.94, J_{ae} = 3.38). These values matched that reported for aloesaponol IV, for which the configuration was established as 2-axial and 4-quasi-axial (Yagi et al., 1977). Aloesaponol IV (**3**) had only been isolated from *A. saponaria* (Yagi et al., 1977), making this the first time it is isolated from another *Aloe* species.

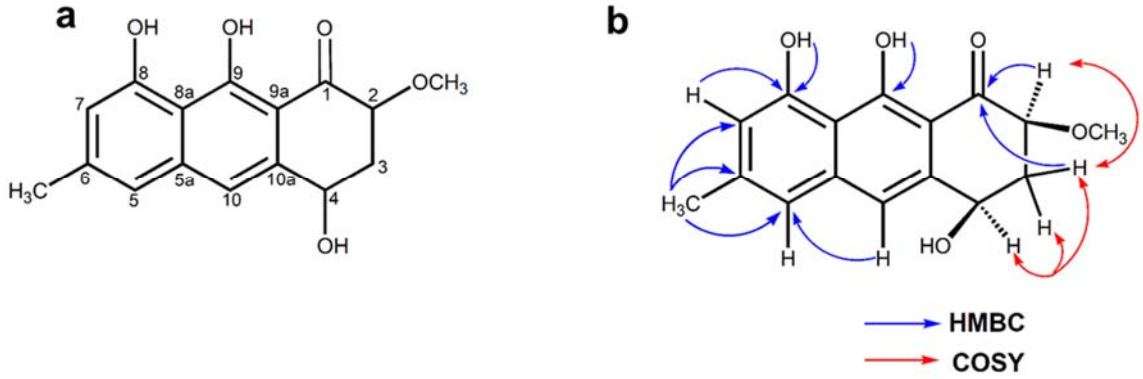

Figure 3: Chemical structure of **a** compound **3**, Aloesaponol IV and **b** selected HMBC and COSY correlations.

Compound **4** was obtained as a white powder. Its molecular formula was established as $C_{13}H_{10}O_4$ on the basis of its QTOF mass spectrum (*m/z* 231.0636 $[M+H]^+$, calcd. for $C_{13}H_{11}O_4$, 231.0657), ^1H and ^{13}C NMR data. The ^1H NMR spectrum showed signal at δ_H 4.41 (3H, s), integrating for three protons, accounting for the presence of a methoxy group. In the aromatic region, three signals appeared at δ_H 7.52 (1H, *t*, *J* = 7.9 Hz, H-6), 7.38 (1H, *d*, *J* = 8.2 Hz, H-7) and 6.93 (1H, *d*, *J* = 7.61 Hz, H-5) displaying an ABC pattern and one at δ_H 7.56 (1H, s, H-4) accounting for the proton on the second ring. A singlet resonating at δ_H 5.38 (2H, s, H-3) was assigned to the

methylene in the naphthalide moiety (see Figure 4). A signal at δ_H 9.73 (1H, s, OH-8) revealed the presence of an aromatic hydroxyl group. Its position was assigned through HMBC interactions of both the hydroxyl group and two aromatic protons belonging to the ABC system (H-5 and H-6) with the carbon appearing at δ_c 156.62 (Figure 4 b). The ^{13}C NMR spectrum displayed a signal at δ_c 168.09, which was assigned as the carbonyl in the naphthalide moiety. COSY correlations between the methylene protons and the aromatic singlet further supported their position (Figure 4). The NMR data for compound **4** matched that previously reported for β-sorigenin-1-*O*-methylether, a semi-synthetic compound derived from the natural product geshoidin (Abegaz and Kebede, 1995).

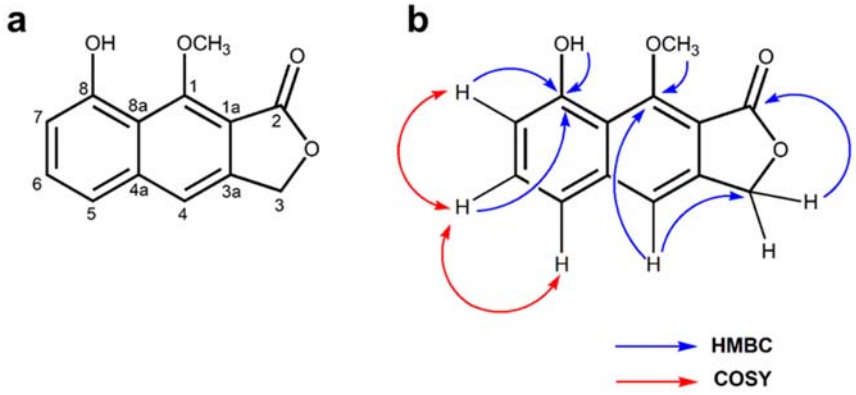

Figure 4: Chemical structure of **a** compound **4**, β-sorigenin-1-*O*-methylether and **b** selected HMBC and COSY correlations.

Compounds **1**, **5** and **6** were identified as the known compounds aloesaponol I (**1**), emodin (**5**) and chrysophanol (**6**), respectively, as their NMR data compared favourably with those reported in the literature (Canche-Escamilla, 2019, Ngan, 2017, Uzun, 2020); The ^{1}H and ^{13}C NMR data are provided in the supplementary file. Chrysophanol (**6**) had been reported as a characteristic component of *Aloe* species roots (Van Wyk et al., 1995). Aloesaponol I (**1**) had been detected in the majority of *Aloe* species subterranean parts, including *A. marlothii* (Van Wyk et al., 1995).

3.4 *In vitro* antiplasmodial activity of isolated compounds against *P. falciparum* (NF54 and K1) ABS parasites

The activity of the isolated compounds was determined against drug sensitive NF54 *P. falciparum* ABS (Table 2). Chloroquine served as a positive control giving an IC_{50} of 0.004 μg/mL (0.008 μM) consistent with prior studies (Verlinden et al., 2011). Compounds **1-5** displayed varied potency against ABS *P. falciparum* ranging from good (IC_{50}<10 μg/mL) to moderate (IC_{50} of 10-50 μg/mL) activity, as per the classification criteria defined by Batista *et al.* (Batista et al., 2009). Aloesaponarin I (**2**) (IC_{50} = 1.56 μg/mL (5.00 μM)) was the most active while β-sorigenin-1-*O*-methylether (**4**) (IC_{50} = 28.97 μg/mL (124.7 μM)) was the least potent. Aloesaponarin I (**2**) was further profiled against multidrug resistant K1 *P. falciparum* ABS, which indicated equipotency (IC_{50} = 1.58 μg/mL (5.06 μM)) with that of NF54 strain (resistance index (RI) = 1.0), implying there is no cross resistance of aloesaponarin I (**2**) across these strains of *P. falciparum*. This schizonticidal activity of aloesaponarin I (**2**) is consistent with an IC_{50} value of 5.58 μM previously reported against another multidrug-resistant *P. falciparum* strain, Dd2 (Hou et al., 2009). However, this data contrasts other reports where aloesaponarin I (**2**) was observed to be 3 to 5-fold less active against ABS from

sulphadoxine and mefloquine resistant D6 and multidrug-resistant W2 *P. falciparum* strains, with IC_{50} values of 25 μM and 16.4 μM, respectively (Abdissa et al., 2017). This diminished potency could be due to multiple factors including strain-specific activity, variation in culturing protocols, incubation periods and assay platforms used. Nonetheless, the fact that aloesaponarin I (**2**) has been identified in the roots of *A. marlothii* may support its traditional application as an antimalarial remedy.

Table 2: ***In vitro*** activity of compounds against *P. falciparum* NF54 ABS parasites

Compound	Activity against *P. falciparum* ABS parasites (IC_{50}, μg/mL)*		RI[∞]
	NF54	K1	
Aloesaponol I (**1**)	10.4 ± 1.4 (42 μM)	ND	ND
Aloesaponarin I (**2**)	1.6 ± 0.7 (5 μM)	1.6± 0.6 (5.1 μM)	1.0
Aloesaponol IV (**3**)	19.8 ± 6.8 (68 μM)	ND	ND
β-sorigenin-1-*O*-methylether (**4**)	29.0 ± 4.7 (125.9 μM)	ND	ND
Emodin (**5**)	11.0 ± 1.4 (40.9 μM)	ND	ND
Chloroquine	0.004 ± 0.001 (0.008 μM)	0.030 ± 0.009 (0.059 μM)	7.4

* $n = 2$, in technical triplicates

[∞] RI = IC_{50} NF54/IC_{50} K1

3.5 *In vitro* gametocytocidal and gametocidal activity of the isolated compounds

The isolated compounds were evaluated *in vitro* against *P. falciparum* (NF54) late-stage (>90%, stage IV/V) gametocytes using a luciferase assay (Reader et al., 2015) (Figure 5). Furthermore, to assess the functional viability of the mature gametocytes following drug exposure, we examined the inhibition of male and female gamete formation in the presence of aloesaponol IV (**3**). Methylene blue served as positive control for all assays demonstrating activity consistent to that reported elsewhere (Delves et al., 2013; Reader et al., 2015). Evaluation of all five compounds at 10 and 20 μg/mL indicated that only aloesaponol IV (**3**) had marked activity against late-stage gametocytes (79% and 88% inhibition of late-stage gametocyte viability at 10 and 20 μg/mL, respectively). None of the other compounds had any appreciable activity, with only emodin (**5**) with ~60% inhibition of late-stage gametocyte viability at 20 μg/mL. This contrasts overall with the ABS activity observed for the compounds, with aloesaponarin I (**2**) therefore only active against ABS parasites and with no transmission-blocking activity. Aloesaponol IV (**3**) showed an IC_{50} = 6.5 μg/mL (22.6 μM)) against late-stage gametocytes, which indicates increased potency to late-stage gametocytes compared to its activity against ABS. This translated to a 94% inhibition (at 20 μg/mL) of male gametocytes exflagellation, a phenotype that was sex-specific since only 37% inhibition female gamete formation was observed under these conditions. Preference towards late-stage gametocytes such as seen with Aloesaponol IV (**3**) has been noted for other plant derived compounds with, for example, the sesquiterpene lactone 1α,4α-dihydroxybishopsolicepolide also more active against late-stage gametocytes compared to ABS parasites (Moyo et al., 2019). Most intriguing is the profound activity of the natural compound lophirone E, isolated from the plant *Lophira lanceolate* (Ochnaceae), which is 100-fold more selective towards late-stage gametocytes compared to asexual stage *P. falciparum* parasites (Lopatriello et al., 2019).

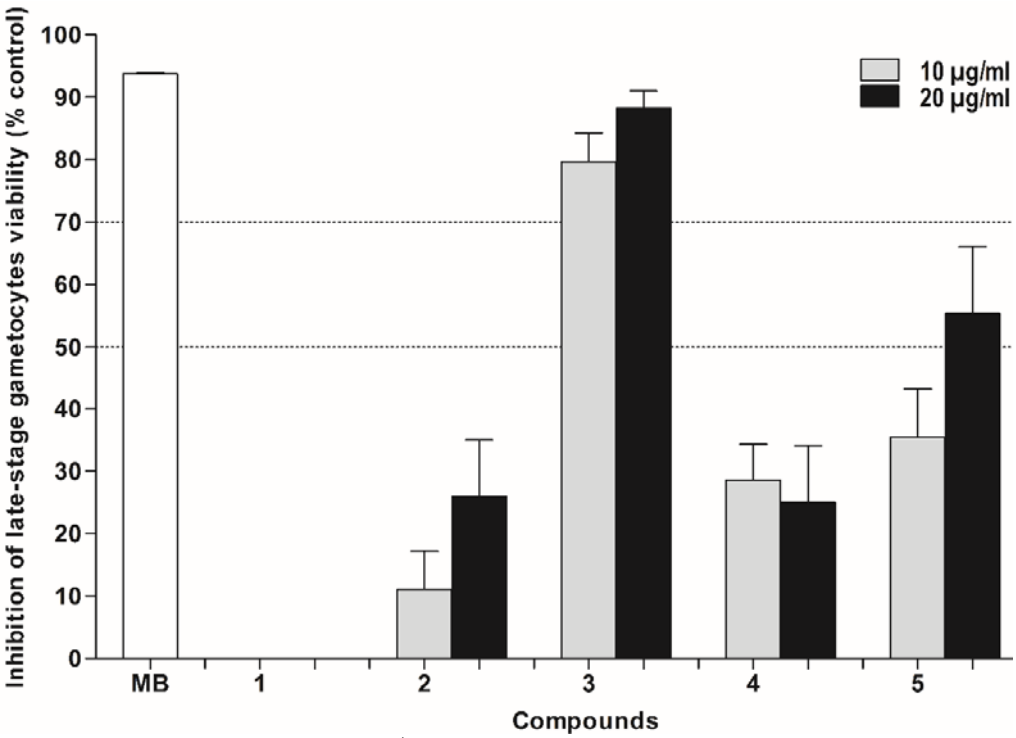

Figure 5: *In vitro* late-stage (>90% stage IV/V) gametocytocidal activity of the isolated compounds. Dual point (10 and 20 µg/mL) (n = 1, in technical triplicates, average ± S.D. indicated) analysis carried out using the luciferase assay. Methylene blue (MB) served as a positive control displaying >90% potency (5 µM).

3.6 Molecular docking

To understand the possible MoA of the most potent compounds against asexual and sexual stage *P. falciparum* parasites, namely aloesaponarin I (**2**) and aloesaponol IV (**3**), respectively, we employed *in silico* predictive tools. Given the existing body of knowledge pointing to anthraquinones as targeting β-hematin polymerisation in *P. falciparum* (Osman and Ismail, 2018), we docked aloesaponarin I (**2**) and the positive control, chloroquine, against the crystal lattice of hemozoin to generate preliminary data to evaluate if this MoA holds true for this compound as well (Figure 6). The favourable binding poses of aloesaponarin I (**2**) were found to have a docking score of -5.463 kcal/mol, ~2-fold lower than that of the more potent positive control chloroquine (-10.004 kcal/mol). In contrast to chloroquine, aloesaponarin I (**2**) interacted with only the fast growing 001 face with no observed docking on the $00\bar{1}$ face (Figure 6). Aloesaponarin I (**2**) possesses significant planarity due to its extensive aromatic moiety which allowed for π-π stacking interactions to exist with the crystal lattice's porphyrin ligands (Figure 6). Interestingly, chloroquine shares similar chemical properties, characteristics which most β-hematin/hemozoin inhibitors possess (Bailly, 2021), which enable them to form the important π-π stacking interactions within the hemozoin crystal lattice – disrupting its ordered polymerisation.

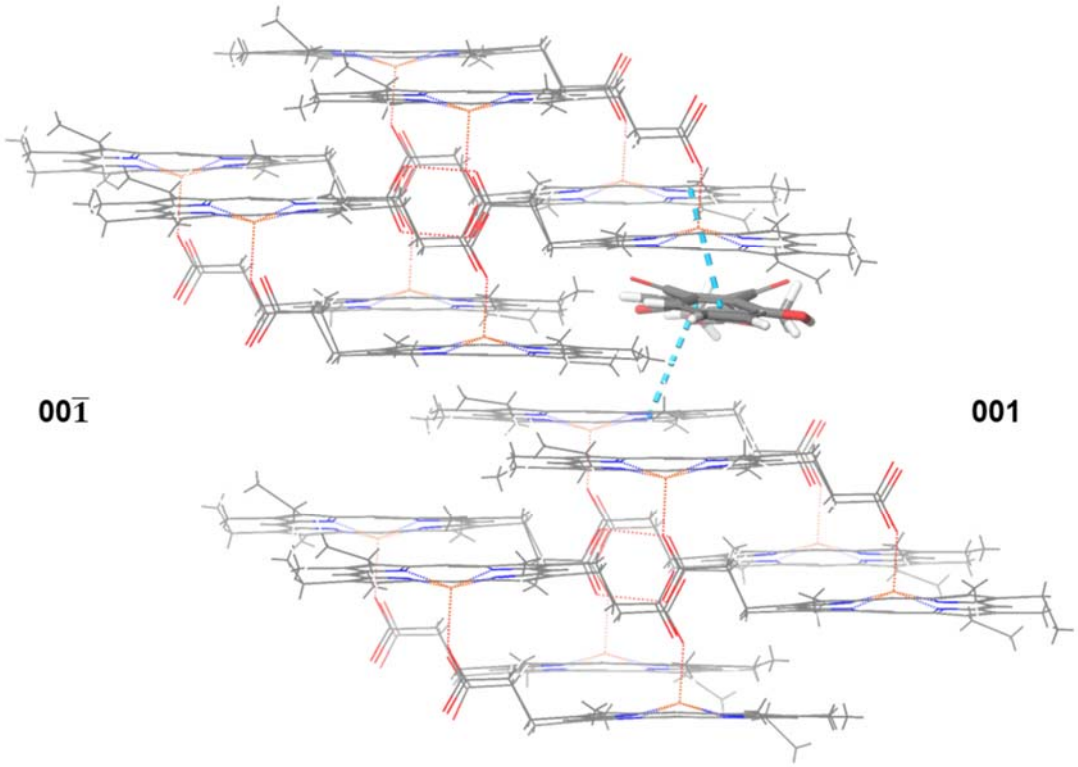

Figure 6: 3D structure of the hemozoin crystal with aloesaponarin I (**2**) exhibiting a preference for docking with the 001 face. π- π stacking interactions (blue) displayed between aloesaponarin I (**2**) and β-hematin crystal structure.

Considering the paucity of knowledge on the MoA of anthraquinones, we used a triangulation method where aloesaponol IV (**3**) was submitted for analysis on two different online target prediction tools, SEA and SuperPred, which have different underlining search approach principles. Hence any common targets independently identified by either tool were speculated to be most likely a biological target for aloesaponol IV. Following the online target prediction, we then validated whether the recognised targets were found in *P. falciparum*. Finally, we then examined the MoA of this compound against its targets using static molecular docking. Interestingly, SEA and SuperPred searches predicted a total of 2 and 123 targets, respectively, with only one common target predicted, DNA topoisomerase II (Supplementary Figure 1). DNA topoisomerase II has generated marked interest as an antimalarial drug target with a dual active compound, pyronaridine, known to target this enzyme in *P. falciparum* (Bailly, 2021; Chavalitshewinkoon-Petmitr et al., 2000). Apart from sharing structural similarities with aloesaponol IV (**3**), pyronaridine demonstrates polypharmacology with added ability to substantially inhibit β-hematin polymerisation in *P. falciparum* (Auparakkitanon et al., 2006). We subsequently docked aloesaponol IV (**3**) and the positive control, pyronaridine, into the crystal structure of *P. falciparum* DNA topoisomerase II (PDB: 6CA8).

Various binding poses were generated for each ligand, in the active site, and visually inspected for favourable interactions. Suitable interactions and poses were observed for aloesaponol IV (**3**) (Figure 7) and pyronaridine within the DNA topoisomerase II binding site. Hydrogen bonds, of acceptable distance ranging from 1.71 to 2.6 Å (Figure 7) (Wu et al., 2012), are noted to form between the Tyr580, Lys650 and Val710 residues and aloesaponol IV (**3**) generating a docking

score of -5.001 kcal/mol. Similarly, pyronaridine was found to dock and interact with the same Val710 residue as aloesaponol IV (**3**), in addition to Glu633, ASN854, Glu856 (Supplementary Figure S1.20), with a comparable docking score of -5.877 kcal/mol.

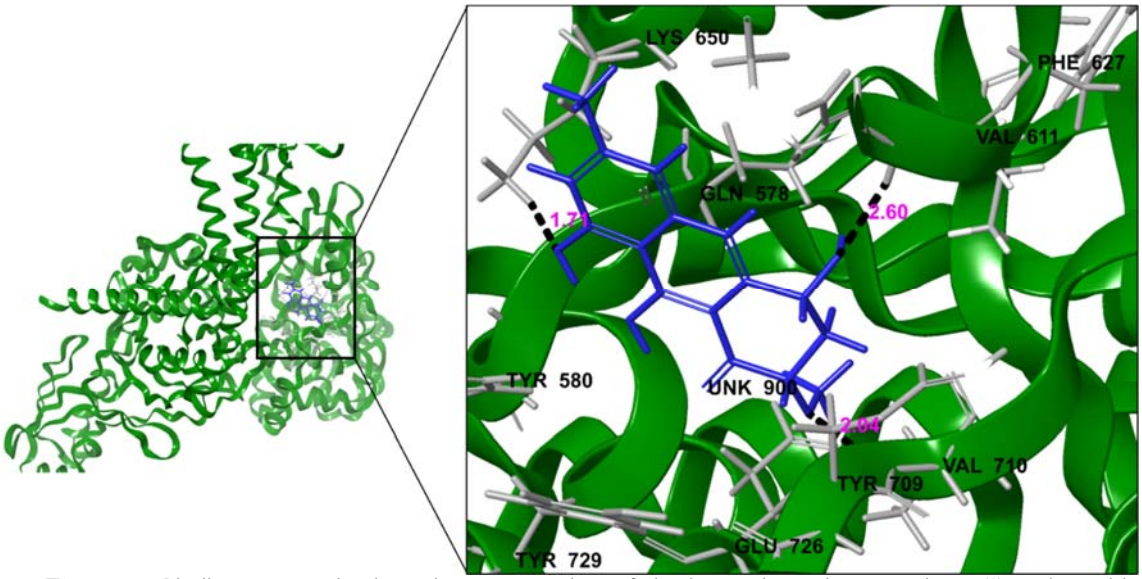

Figure 7: Binding pose and schematic representation of the interactions aloesaponol IV (**3**) makes with surrounding residues of the DNA topoisomerase II enzyme.

Considering the number and type of interactions observed, in comparison to the positive controls, it is likely that aloesaponarin I (**2**) and aloesaponol IV (**3**) bind to β-hematin and DNA topoisomerase II, respectively, lending some explanation to the experimentally observed activity, however, further experimental investigation is required to validate this *in silico* data.

4 Conclusion

The antiplasmodial investigation of *A. marlothii* roots led to the isolation of chemical constituents with anthraquinone or pre-anthraquinone moieties and one naphthalene derivative displaying varied antiplasmodial activities against the sexual and asexual stage of *P. falciparum*. Aloesaponarin I (**2**) was the most active compound against the asexual stage of *P. falciparum*, while aloesaponol IV (**3**) showed the best activity against the gametocytes and male gamete formation. This is the first time that β-sorigenin-1-*O*-methylether has been isolated from an *Aloe* species. Collectively, our study provides tentative data supporting the traditional use of *A. marlothii* for malaria treatment. It has provided first report on the potential transmission-blocking activity from an *Aloe* species while also providing insights into possible MoA of the active compounds.

suAcknowledgment

The authors would like to thank Mr. J. Sampson (Curator at Manie van der Schijff Botanical Garden at the University of Pretoria) and Magda Nel (Herbarium Assistant at Schweickerdt Herbarium, PRU) for their assistance in plant identification, collection and voucher specimen preparation. We are grateful to Dr. Madelien Wooding in running the samples on UPLC-QTOF-MS instrument. Access to the Schrödinger software suite was provided by the CSIR's Center for High Performance Computing (CHPC). This research work was supported by a grant from the Department of Science and Innovation (DSI) of South Africa awarded to Vinesh Maharaj. It was

further supported by the South African Research Chairs Initiative of the DSI, administered through the South African National Research Foundation (UID 84627) and the South African Medical Research Council to Lyn-Marié Birkholtz. The UP ISMC acknowledges the South African Medical Research Council as Collaborating Centre for Malaria Research. Sephora Mutombo Mianda was supported by funds from the University of Pretoria Postgraduate Research Support Bursary, South Africa and the L'Oréal-UNESCO for Woman in Science grant.

Conflict of Interest Statement

The authors declare that there is no conflict of interest.

Credit Authorship Statement

Sephora Mutombo Mianda: data curation, formal analysis, methodology, validation, writing—original draft; **Luke Invernizzi**: docking studies of compounds 2 and 3, writing-original draft; **Mariette E. Botha**: Transmission-blocking testing of compound 3; **Janette Reader**: Gametocytocidal testing of isolated compounds; **Phanankosi Moyo**: data curation, supervision, writing-original draft; **Lyn-Marié Birkholtz**: conceptualization, funding acquisition, investigation, project administration, writing-review and editing; **Vinesh J. Maharaj**: conceptualization, funding acquisition, investigation, project administration, supervision, writing-review and editing.

References

Abdissa, D., Geleta, G., Bacha, K., Abdissa, N., 2017. Phytochemical investigation of *Aloe pulcherrima* roots and evaluation for its antibacterial and antiplasmodial activities. PLoS One 12(3), e0173882.

Alonso, P.L., Brown, G., Arevalo-Herrera, M., Binka, F., Chitnis, C., Collins, F., Doumbo, O.K., Greenwood, B., Hall, B.F., Levine, M.M., Mendis, K., Newman, R.D., Plowe, C.V., Rodríguez, M.H., Sinden, R., Slutsker, L., Tanner, M., 2011. A research agenda to underpin malaria eradication. PLoS medicine 8(1), e1000406.

Amoo, S.O., Aremu, A.O., Van Staden, J., 2014. Unraveling the medicinal potential of South African *Aloe* species. Journal of Ethnopharmacology 153(1), 19-41.

Auparakkitanon, S., Chapoomram, S., Kuaha, K., Chirachariyavej, T., Wilairat, P., 2006. Targeting of hematin by the antimalarial pyronaridine. Antimicrobial Agents and Chemotherapy 50(6), 2197-2200.

Bailly, C., 2021. Pyronaridine: An update of its pharmacological activities and mechanisms of action. Biopolymers 112(4), e23398.

Batista, R., De Jesus Silva Júnior, A., De Oliveira, A.B., 2009. Plant-derived antimalarial agents: new leads and efficient phytomedicines. Part II. Non-alkaloidal natural products. Molecules 14(8), 3037-3072.

Bbosa, G.S., Kyegombe, D.B., Lubega, A., Musisi, N., Ogwal-Okeng, J., Odyek, O., 2013. Anti-*Plasmodium falciparum* activity of *Aloe dawei* and *Justicia betonica*. African Journal of Pharmacy and Pharmacology 7(31), 2258-2263

Birkholtz, L.-M., Alano, P., Leroy, D., 2022. Transmission-blocking drugs for malaria elimination. Trends in Parasitology.

Birkholtz, L.-M., Coetzer, T.L., Mancama, D., Leroy, D., Alano, P., 2016. Discovering new transmission-blocking antimalarial compounds: challenges and opportunities. Trends in Parasitology 32(9), 669-681

Bohle, D.S., Dodd, E.L., Stephens, P.W., 2012. Structure of malaria pigment and related propanoate-linked metalloporphyrin.pdf. Chemistry & Biodiversity 9(9), 1891-1902.

Burrows, J.N., Duparc, S., Gutteridge, W.E., Hooft van Huijsduijnen, R., Kaszubska, W., Macintyre, F., Mazzuri, S., Möhrle, J.J., Wells, T.N.C., 2017. New developments in anti-malarial target candidate and product profiles. Malaria Journal 16(1), 26.

Canche-Escamilla, G., Colli-Acevedo, P., Borges-Argaez, R., Quintana-Owen, P., May-Crespo, J.F., Cáceres-Farfan, M., Yam Puc, J.A., Sansores-Peraza, P., Vera-Ku, B.M., 2019. Extraction of phenolic components from an *Aloe vera* (*Aloe barbadensis* Miller) crop and their potential as antimicrobials and textile dyes. Sustainable Chemistry and Pharmacy 14, 100168.

Chavalitshewinkoon-Petmitr, P., Pongvilairat, G., Auparakkitanon, S., Wilairat, P., 2000. Gametocytocidal activity of pyronaridine and DNA topoisomerase II inhibitors against multidrug-resistant *Plasmodium falciparum in vitro*. Parasitology International 48(4), 275-280.

Clarkson, C., Maharaj, V.J., Crouch, N.R., Grace, O.M., Pillay, P., Matsabisa, M.G., Bhagwandin, N., Smith, P.J., Folb, P.I., 2004. *In vitro* antiplasmodial activity of medicinal plants native to or naturalised in South Africa. Journal of Ethnopharmacology 92(2), 177-191.

Cox, F.E., 2010. History of the discovery of the malaria parasites and their vectors. Parasites & Vectors 3(1), 1-9.

Dagne, E., Yenesew, A., Asmellash, S., Demissew, S., Mavi, S., 1994. Anthraquinones, pre-anthraquinones and isoeleutherol in the roots of *Aloe* species. Phytochemistry 35(2), 401-406.

de Wet, H., Ramulondi, M., Ngcobo, Z.N., 2016. The use of indigenous medicine for the treatment of hypertension by a rural community in northern Maputaland, South Africa. South African Journal of Botany 103, 78-88.

Delves, M.J., Ruecker, A., Straschil, U., Lelièvre, J., Marques, S., López-Barragán, M.J., Herreros, E., Sinden, R.E., 2013. Male and female *Plasmodium falciparum* mature gametocytes show different responses to antimalarial drugs. Antimicrobial Agents and Chemotherapy 57(7), 3268-3274.

Deressa, T., Mekonnen, Y., Animut, A., 2010. *In vivo* anti-malarial activities of *Clerodendrum myricoides*, *Dodonea angustifolia* and *Aloe debrana* against *Plasmodium berghei*. Ethiopian Journal of Health Development 24(1).

Dibessa, T.T., Engidawork, E., Nedi, T., Teklehaymanot, T., 2020. Antimalarial activity of the aqueous extract of the latex of *Aloe pirottae* Berger. (Aloaceae) against *Plasmodium berghei* in mice. Journal of Ethnopharmacology 255, 112763.

Erasmus, L.J.C., Potgieter, M.J., Semenya, S.S., Lennox, S.J., 2012. Phytomedicine versus gonorrhoea: The Bapedi experience. African Journal of Traditional, Complementary and Alternative Medicines 9(4), 591-598.

Friesner, R.A., Murphy, R.B., Repasky, M.P., Frye, L.L., Greenwood, J.R., Halgren, T.A., Sanschagrin, P.C., Mainz, D.T., 2006. Extra precision glide: docking and scoring incorporating a model of hydrophobic enclosure for protein-ligand complexes. Journal of Medicinal Chemistry 49(21), 6177–6196.

Geremedhin, G., Bisrat, D., Asres, K., 2014. Isolation, characterization and *in vivo* antimalarial evaluation of anthrones from the leaf latex of *Aloe percrassa* Todaro. Journal of Natural Remedies 14(2), 119-125.

Greenwood, J.R., Calkins, D., Sullivan, A.P., Shelley, J.C., 2010. Towards the comprehensive, rapid, and accurate prediction of the favorable tautomeric states of drug-like molecules in aqueous solution. Journal of Computer-aided Molecular Design 24(6-7), 591-604.

Hintsa, G., Sibhat, G.G., Karim, A., 2019. Evaluation of antimalarial activity of the leaf latex and TLC isolates from *Aloe megalacantha* Baker in *Plasmodium berghei* infected mice. Evidence-Based Complementary and Alternative Medicine 2019, 6459498.

Hou, Y., Cao, S., Brodie, P.J., Callmander, M.W., Ratovoson, F., Rakotobe, E.A., Rasamison, V.E., Ratsimbason, M., Alumasa, J.N., Roepe, P.D., Kingston, D.G.I., 2009. Antiproliferative

and antimalarial anthraquinones of *Scutia myrtina* from the Madagascar forest. Bioorganic & Medicinal Chemistry 17(7), 2871-2876.

Huy, N.T., Chi, P.L., Nagai, J., Dang, T.N., Mbanefo, E.C., Ahmed, A.M., Long, N.P., Thoa, L.T.B., Hung, L.P., Titouna, A., 2017. High-throughput screening and prediction model building for novel hemozoin inhibitors using physicochemical properties. Antimicrobial Agents and Chemotherapy 61(2), e01607-01616.

Jacobson, M.P., Friesner, R.A., Xiang, Z., Honig, B., 2002. On the role of the crystal environment in determining protein side-chain conformations. Journal of Molecular Biology 320(3), 597–608.

Jacobson, M.P., Pincus, D.L., Rapp, C.S., Day, T.J.F., Honig, B., Shaw, D.E., Friesner, R.A., 2004. A hierarchical approach to all-atom protein loop prediction. Proteins: Structure, Function, and Bioinformatics 55(2), 351–367.

Johnson, J.D., Dennull, R.A., Gerena, L., Lopez-Sanchez, M., Roncal, N.E., Waters, N.C., 2007. Assessment and continued validation of the malaria SYBR Green I-based fluorescence assay for use in malaria drug screening. Antimicrobial Agents and Chemotherapy 51(6), 1926-1933.

Keiser, M.J., Roth, B.L., Armbruster, B.N., Ernsberger, P., Irwin, J.J., Shoichet, B.K., 2007. Relating protein pharmacology by ligand chemistry. Nature Biotechnology 25(2), 197-206.

Khunoana, E.T., Madikizela, B., Erhabor, J.O., Nkadimeng, S.M., Arnot, L.F., Van Wyk, I., McGaw, L.J., 2019. A survey of plants used to treat livestock diseases in the Mnisi community, Mpumalanga, South Africa, and investigation of their antimicrobial activity. South African Journal of Botany 126, 21-29.

Lopatriello, A., Sore, H., Habluetzel, A., Parapini, S., D'Alessandro, S., Taramelli, D., Taglialatela-Scafati, O., 2019. Identification of a potent and selective gametocytocidal antimalarial agent from the stem barks of *Lophira lanceolata*. Bioorganic Chemistry 93, 103321.

Mosaddeque, F., Mizukami, S., Kamel, M.G., Teklemichael, A.A., Dat, T.V., Mizuta, S., Toan, D.V., Ahmed, A.M., Vuong, N.L., Elhady, M.T., 2018. Prediction model for antimalarial activities of hemozoin inhibitors by using physicochemical properties. Antimicrobial Agents and Chemotherapy 62(5), e02424-02417.

Moyo, P., Botha, M.E., Nondaba, S., Niemand, J., Maharaj, V.J., Eloff, J.N., Louw, A.I., Birkholtz, L., 2016. *In vitro* inhibition of *Plasmodium falciparum* early and late stage gametocyte viability by extracts from eight traditionally used South African plant species. Journal of Ethnopharmacology 185, 235-242.

Moyo, P., Kunyane, P., Selepe, M.A., Eloff, J.N., Niemand, J., Louw, A.I., Maharaj, V.J., Birkholtz, L.-M., 2019. Bioassay-guided isolation and identification of gametocytocidal compounds from *Artemisia afra* (Asteraceae). Malaria Journal 18(1), 1-11.

Moyo, P., Mugumbate, G., Eloff, J.N., Louw, A.I., Maharaj, V.J., Birkholtz, L.-M., 2020. Natural products: a potential source of malaria transmission blocking drugs? Pharmaceuticals 13(9), 251.

Mulyangote, L.T., 2016. Ethnobotany and bioactivity of medicinal plants used to treat symptoms associated with gastro-intestinal infections in Namibia. MSc thesis, University of Namibia.

Ndlela, S.Z., Mkwanazi, M.V., Chimonyo, M., 2021. *In vitro* efficacy of plant extracts against gastrointestinal nematodes in goats. Tropical Animal Health and Production 53(2), 295.

Ngan, N.T.T., Quang, T.H., Kim, K.-W., Kim, H.J., Sohn, J.H., Kang, D.G., Lee, H.S., Kim, Y.-C., Oh, H., 2017. Anti-inflammatory effects of secondary metabolites isolated from the marine-derived fungal strain *Penicillium* sp. SF-5629. Archives of Pharmacal Research 40(3), 328-337.

Nguta, J., Mbaria, J., Gakuya, D., Gathumbi, P., Kiama, S., 2010. Traditional antimalarial phytotherapy remedies used by the South Coast community, Kenya. Journal of Ethnopharmacology 131(2), 256-267.

Nickel, J., Gohlke, B.-O., Erehman, J., Banerjee, P., Rong, W.W., Goede, A., Dunkel, M., Preissner, R., 2014. SuperPred: update on drug classification and target prediction. Nucleic Acids Research 42(W1), W26-W31.

Nicosia, E., Valenti, R., Guillet, A., Malatesta, L., Tallone, G., Mondlane, T.D.S.M., Attorre, F., 2020. ABS provides opportunities for indigenous and local communities in the Limpopo National Park. An ethnobotanical survey of plants used by the Changana community, Limpopo National Park, Mozambique.

Osman, C.P., Ismail, N.H., 2018. Antiplasmodial anthraquinones from medicinal plants: the chemistry and possible mode of actions. Natural Product Communications 13(12), 1934578X1801301207.

Pagola, S., Stephens, P.W., Bohle, D.S., Kosar, A.D., Madsen, S.K., 2000. The structure of malaria pigment β-haematin. Nature 404, 307–310.

Paulos, B., Bisrat, D., Gedif, T., Asres, K., 2011. Antimalarial and antioxidant activities of the leaf exudates and a naphthalene derivative from *Aloe otallensis* Baker. Ethiopian Pharmaceutical Journal 29(2), 100-107.

Reader, J., Botha, M., Theron, A., Lauterbach, S.B., Rossouw, C., Engelbrecht, D., Wepener, M., Smit, A., Leroy, D., Mancama, D., 2015. Nowhere to hide: interrogating different metabolic parameters of *Plasmodium falciparum* gametocytes in a transmission blocking drug discovery pipeline towards malaria elimination. Malaria Journal 14(1), 1-17.

Reader, J., van der Watt, M.E., Taylor, D., Le Manach, C., Mittal, N., Ottilie, S., Theron, A., Moyo, P., Erlank, E., Nardini, L., 2021. Multistage and transmission-blocking targeted antimalarials discovered from the open-source MMV Pandemic Response Box. Nature Communications 12(1), 1-15.

Ribeiro, A., Romeiras, M.M., Tavares, J., Faria, M.T., 2010. Ethnobotanical survey in Canhane village, district of Massingir, Mozambique: medicinal plants and traditional knowledge. Journal of Ethnobiology and Ethnomedicine 6(1), 33.

Ruecker, A., Mathias, D.K., Straschil, U., Churcher, T.S., Dinglasan, R.R., Leroy, D., Sinden, R.E., Delves, M.J., 2014. A male and female gametocyte functional viability assay to identify biologically relevant malaria transmission-blocking drugs. Antimicrobial Agents and Chemotherapy 58(12), 7292-7302.

SANBI, 2007. *Aloe marlothii* A.Berger. http://pza.sanbi.org/aloe-marlothii. (Accessed September 2021).

Sato, S., 2021. *Plasmodium*—a brief introduction to the parasites causing human malaria and their basic biology. Journal of Physiological Anthropology 40(1), 1-13.

Schmelzer, G., Gurib-Fakim, A., 2008. Plant resources of Tropical Africa 11 (1). Medicinal plants 1. PROTA Foundation, Wageningen, Netherlands. Backhuys Publishers, Leiden, Netherlands/CTA, Wageningen, Netherlands.

Semenya, S., Potgieter, M., Erasmus, L., 2012. Ethnobotanical survey of medicinal plants used by Bapedi healers to treat diabetes mellitus in the Limpopo Province, South Africa. Journal of Ethnopharmacology 141(1), 440-445.

Semenya, S.S., Mokgoebo, M.J., 2020. The utilization and conservation of indigenous wild plant resources in the Limpopo Province, South Africa, Natural Resources Management and Biological Sciences. IntechOpen.

Shelley, J.C., Cholleti, A., Frye, L.L., Greenwood, J.R., Timlin, M.R., Uchimaya, M., 2007. Epik: A software program for pKa prediction and protonation state generation for drug-like molecules. Journal of Computer-Aided Molecular Design 21, 681–691.

Sinha, A., Hughes, K.R., Modrzynska, K.K., Otto, T.D., Pfander, C., Dickens, N.J., Religa, A.A., Bushell, E., Graham, A.L., Cameron, R., Kafsack, B.F.C., Williams, A.E., Llinás, M.,

Berriman, M., Billker, O., Waters, A.P., 2014. A cascade of DNA-binding proteins for sexual commitment and development in *Plasmodium*. Nature 507(7491), 253-257.

Smilkstein, M., Sriwilaijaroen, N., Kelly, J.X., Wilairat, P., Riscoe, M., 2004. Simple and inexpensive fluorescence-based technique for high-throughput antimalarial drug screening. Antimicrobial Agents and Chemotherapy 48(5), 1803-1806.

Sol Sol de Medeiros, D., Tasca Cargnin, S., Azevedo dos Santos, A.P., de Souza Rodrigues, M., Berton Zanchi, F., Soares de Maria de Medeiros, P., de Almeida e Silva, A., Bioni Garcia Teles, C., Baggio Gnoatto, S.C., 2021. Ursolic and betulinic semisynthetic derivatives show activity against CQ-resistant *Plasmodium falciparum* isolated from Amazonia. Chemical Biology & Drug Design 97(5), 1038–1047.

Teka, T., Awgichew, T., Kassahun, H., 2020. Antimalarial activity of the leaf latex of *Aloe weloensis* (Aloaceae) against *Plasmodium berghei* in mice. Journal of Tropical Medicine 2020, 1397043.

Teka, T., Bisrat, D., Yeshak, M.Y., Asres, K., 2016. Antimalarial activity of the chemical constituents of the leaf latex of *Aloe pulcherrima* Gilbert and Sebsebe. Molecules 21(11), 1415.

Tewabe, Y., Assefa, S., 2018. Antimalarial potential of the leaf exudate of *Aloe macrocarpa* todaro and its major constituents against *Plasmodium berghei*. Clinical Experiment of Pharmacology 8(1), 2161-1459.

Uzun, M., Guvenalp, Z., Kazaz, C., Demirezer, L.O., 2020. Matrix metalloproteinase inhibitor and sunscreen effective compounds from *Rumex crispus* L.: isolation, identification, bioactivity and molecular docking study. Phytochemical Analysis 31(6), 818-834

Van Wyk, B.-E., Yenesew, A., Dagne, E., 1995. Chemotaxonomic survey of anthraquinones and pre-anthraquinones in roots of *Aloe* species. Biochemical Systematics and Ecology 23(3), 267-275.

van Zyl, R.L., Viljoen, A.M., Jäger, A.K., 2002. *In vitro* activity of *Aloe* extracts against *Plasmodium falciparum*. South African Journal of Botany 68(1), 106-110.

Verlinden, B.K., Niemand, J., Snyman, J., Sharma, S.K., Beattie, R.J., Woster, P.M., Birkholtz, L.-M., 2011. Discovery of novel alkylated (bis)urea and (bis)thiourea polyamine analogues with potent antimalarial activities. Journal of Medicinal Chemistry 54(19), 6624-6633.

Wabuyele, E., Kyalo, S., 2008. Sustainable use of East African aloes: the case of commercial aloes in Kenya, International Workshop on the Convention of International Trade in Endangered Species of Wild Fauna and Flora.

Wanjohi, J.M., 2005. Antiplasmodial anthracene derivatives from some Kenyan *Aloe* and *Bulbine* species. PhD thesis, Univcersity of Nairobi.

Warhurst, D.C., Craig, J.C., Adagu, I.S., Meyer, D.J., Lee, S.Y., 2003. The relationship of physico-chemical properties and structure to the differential antiplasmodial activity of the cinchona alkaloids. Malaria Journal 2(1), 1-14.

Wells, T.N., 2011. Natural products as starting points for future anti-malarial therapies: going back to our roots? Malaria Journal 10(1), 1-12.

WHO, 2021. World malaria report 2021. Geneva. Licence: CC BY-NC-SA 3.0 IGO..

Wu, C.C., Li, Y.C., Wang, Y.R., Li, T.K., Chan, N.L., 2013. On the structural basis and design guidelines for type II topoisomerase-targeting anticancer drugs. Nucleic Acids Research 41, 10630–10640.

Wu, M.Y., Dai, D.Q., Yan, H., 2012. PRL-dock: Protein-ligand docking based on hydrogen bond matching and probabilistic relaxation labeling. Proteins: Structure, Function, and Bioinformatics 80(9), 2137-2153.

Yagi, A., Makino, K., Nishioka, I., 1977. Studies on the constituents of *Aloe saponaria* HAW. II. The structures of tetrahydroanthracene derivatives, aloesaponol III and -IV. Chemical & Pharmaceutical Bulletin 25(7), 1764-1770.

Yenesew, A., Ogur, J.A., Duddeckt, H., 1993. (R)-Prechrysophanol from *Aloe graminicola*. Phytochemistry 34(5), 1442-1444.